

Micro- and Nanotechnology for Biomedical and Environmental Applications

Raymond P. Mariella, Jr.
Chair/Editor

**26-27 January 2000
San Jose, California, USA**

Sponsored by
U.S. Air Force Office of Scientific Research
SPIE – The International Society for Optical Engineering
IBOS – International Biomedical Optics Society

**Proceedings of SPIE
Volume 3912**

73.64
R263

PROGRESS IN BIOMEDICAL OPTICS

Vol. 1, No. 6

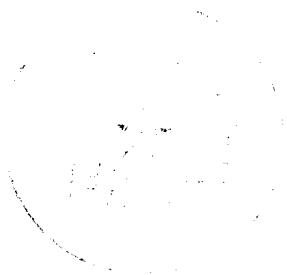
Micro- and Nanotechnology for Biomedical and Environmental Applications

Raymond P. Mariella, Jr.
Chair/Editor

26-27 January 2000
San Jose, California, USA

Sponsored by
U.S. Air Force Office of Scientific Research
SPIE – The International Society for Optical Engineering
IBOS – International Biomedical Optics Society

Published by
SPIE – The International Society for Optical Engineering



Proceedings of SPIE
Volume 3912

SPIE is an international technical society dedicated to advancing engineering and scientific applications of optical, photonic, imaging, electronic, and optoelectronic technologies.

2015016



2-14/04

The papers appearing in this book compose the proceedings of the technical conference cited on the cover and title page of this volume. They reflect the authors' opinions and are published as presented, in the interests of timely dissemination. Their inclusion in this publication does not necessarily constitute endorsement by the editors or by SPIE. Papers were selected by the conference program committee to be presented in oral or poster format, and were subject to review by volume editors or program committees.

Please use the following format to cite material from this book:

Author(s), "Title of paper," in *Micro- and Nanotechnology for Biomedical and Environmental Applications*, Raymond P. Mariella, Jr., Editor, Proceedings of SPIE Vol. 3912, page numbers (2000).

ISSN 1017-2661
ISBN 0-8194-3528-7

Published by
SPIE—The International Society for Optical Engineering
P.O. Box 10, Bellingham, Washington 98227-0010 USA
Telephone 360/676-3290 (Pacific Time) • Fax 360/647-1445

Copyright ©2000, The Society of Photo-Optical Instrumentation Engineers.

Copying of material in this book for internal or personal use, or for the internal or personal use of specific clients, beyond the fair use provisions granted by the U.S. Copyright Law is authorized by SPIE subject to payment of copying fees. The Transactional Reporting Service base fee for this volume is \$15.00 per article (or portion thereof), which should be paid directly to the Copyright Clearance Center (CCC), 222 Rosewood Drive, Danvers, MA 01923. Payment may also be made electronically through CCC Online at <http://www.directory.net/copyright/>. Other copying for republication, resale, advertising or promotion, or any form of systematic or multiple reproduction of any material in this book is prohibited except with permission in writing from the publisher. The CCC fee code is 1017-2661/00/\$15.00.

Printed in the United States of America.

Conference Committee

Conference Chair

Raymond P. Mariella, Jr., Lawrence Livermore National Laboratory

Cochair

Tejal A. Desai, University of Illinois/Chicago

Program Committee

Harold G. Craighead, Cornell University

Paul L. Gourley, Sandia National Laboratories

Yuji Kikuchi, National Food Research Institute (Japan)

Raoul Kopelman, University of Michigan

Peter A. Krulevitch, Lawrence Livermore National Laboratory

Makarand Paranjape, Georgetown University

Ian T. Young, Delft University of Technology (Netherlands)

Session Chairs

- 1 BioMEMS for Diagnostics and Biosensing
 Yuji Kikuchi, National Food Research Institute (Japan)
- 2 Cell- and Protein-based Microtechnology
 Paul L. Gourley, Sandia National Laboratories
- 3 Fabrication and Characterization of BioMEMS
 Raymond P. Mariella, Jr., Lawrence Livermore National Laboratory
- 4 Analytical Applications of BioMEMS
 Ian T. Young, Delft University of Technology (Netherlands)

Introduction

This year's conference, as has been its tradition, was an international conference. As microtechnology has matured, the breadth of its applications has increased. In this year's conference there were presentations covering in-vivo applications and rapid detection of glioblastoma (cancerous) cells, direct kinetic (sub-one-minute) measurements of antibody-antigen binding, RNA detection, miniaturized cell-based bioassays, highly parallel microchannel arrays for cell studies, growth and manipulation of endothelial cells, 3D tomography using acousto-optical coupling techniques, tribological wear, and chemical/mechanical polishing using atomic-force microscopy— just to name a few!

In addition to the applications, we heard about a wide variety of fabrication technologies that enable the applications, including LIGA to fabricate miniature replicated grating spectrometers that match photonic systems using fiber optics, several guided-wave or leaky-mode optical techniques for analyses, and patterning of proteins and fibroblasts on surfaces. Micro- and nanocavities and pipettes were also described.

State-of-the-art hardware technologies were also presented, including fiber optic coupling and wavelength filtering and merging, along with an actuator that moved centimeter distances with micron precision.

Raymond P. Mariella, Jr.

Summary of Discussion on BioMEMS-based Instrumentation

A formal presentation had to be withdrawn, so the conference chairman initiated an audience participation discussion which addressed his Saturday night "Hot Topics" subject, "Individualized medicine: the future of bioMEMS."

The recent focus of micro-electro-mechanical systems (MEMS) -based instrumentation has dealt largely with increasing the throughput of established processes, including drug screening/drug discovery/combinatorial chemistry, or the miniaturization of accepted bench-top instruments. The miniaturization and automation of procedures that were previously performed manually is included in these activities. For example, hand-held — or at least portable — instruments that run real-time polymerase chain reaction (PCR) in under 10 minutes and perform varying levels of automated sample preparation for PCR, including the Taqman® assays, are now available.

The concept posed to the audience was whether the future of bioMEMS instrumentation might adopt an additional direction, that of providing information and capabilities to the physician that are not available today. In particular, researchers from the Center for Disease Control and Prevention, Influenza Branch, have said that it would be valuable for physicians to be able to determine the genomic sequences of polymorphic regions for the strain(s) of influenza that infect our population. Each year, the CDC would look at foreign strains that have just appeared (for example, in Asia), and then prepare a vaccine against such a strain. As winter arrives and as soon as cases start to appear, they would try to determine if there is a match between the vaccine that they have distributed and the flu strain(s) that are spreading through the population.

The Plan

One generalized near-term goal for bioMEMS-based instrumentation would be to determine the ailment of a patient while he/she is in the physician's office:

- viral
- bacterial (antibiotic resistance or susceptibility, etc.)
- parasitic
- none of the above.

This requires the physician to have the ability to detect and determine the nucleic-acid sequences of the relevant organisms and to have a (web-based?) network over which the information may be exchanged in a timely fashion.

A longer-term goal would be the selection of treatment based on the genetics of each patient. This is a formidable technical challenge, but many of the required capabilities

are being developed already. This requires knowledge of the human genome and its polymorphisms. It requires a profound understanding of functional genomics—the relationship between an individual's genome and external stimuli (the regulation of gene expression, the role of the proteins being synthesized, etc.). If attained, the results could be very beneficial:

- Armed with genetic information about infections and the patient, and after determining the biomarkers for allergies, exposure to toxins, as well as those for infections, the physician could select which medicines/treatments would be the most efficacious.
- The physician could avoid medicines that would have undesirable side effects in a patient.

In order to achieve such a capability, science and technology need to make major advances; it is evident from the presentations in this conference and in others at BiOS 2000 that many researchers are moving in the necessary directions. The revolution in information technology also promises to provide the enormous increases in the bandwidth of information access and exchange that will be necessary to deliver such capabilities into the offices of physicians and clinics. One existing reason that the cost of drug development is high is that a drug will be rejected in its final trials if a fraction of the cohort being studied shows sufficiently adverse reactions. The hope is that the genetic makeup of those who experience benefits from a drug may be delineated from those showing adverse reactions. This will permit the application of this drug to that fraction of the population that it will benefit. In the distant future, the science of functional genomics and proteomics may even permit the prediction of beneficial and adverse effects!

After these statements, the audience commented.

A physician in the audience commented that he thought moving toward individualized medicine was moving in the right direction, but also commented on the risk of information overload, and the need for an "expert system" to assist the physicians in the use of such a complex databank/diagnostic function.

The need for, and difficulty of the genomics issues were reflected upon by several in the audience.

Comments on the "information superhighway" were made, along with comments about the recent advances by numerous organizations in sample collection, sample preparation, and assays, using miniaturized instruments.

Raymond P. Mariella, Jr.

Contents

vii	Conference Committee
ix	Introduction

SESSION 1 BIOMEMS FOR DIAGNOSTICS AND BIOSENSING

- 2 **Detecting cancer quickly and accurately [3912-01]**
P. L. Gourley, A. E. McDonald, J. K. Hendricks, G. C. Copeland, J. A. Hunter, O. Akhil, D. Cheung, J. Cox, Sandia National Labs.; H. Capps, M. S. Curry, S. L. Skirboll, Univ. of New Mexico School of Medicine
- 11 **Optoelectronic microdevices for combined phototherapy [3912-02]**
V. P. Zharov, Yu. A. Menyaev, V. A. Hamaev, G. M. Antropov, Bauman Moscow State Univ. of Technology (Russia); M. Waner, Univ. of Arkansas for Medical Sciences
- 23 **Nanoscale microcavities for biomedical sensor applications [3912-04]**
S. Chan, P. M. Fauchet, Y. Li, L. J. Rothberg, Univ. of Rochester
- 35 **Multicolor fluorescence detection of ribosomal RNA in microchannels [3912-05]**
M. Balberg, K. Hristova, Univ. of Illinois/Urbana-Champaign; M. Mau, Technische Univ. Freiberg (Germany); D. Frigon, H. C. Zeringue, D. J. Brady, D. J. Beebe, L. Raskin, Univ. of Illinois/Urbana-Champaign
- 41 **Micromachined pipettes integrated in a flow channel for single DNA molecule study by optical trapping [3912-06]**
C. R. Rusu, R. van't Oever, M. J. de Boer, H. V. Jansen, E. Berenschot, M. C. Elwenspoek, M. L. Bennink, J. S. Kanger, B. G. de Grooth, J. Greve, J. Brugger, A. van den Berg, Univ. of Twente (Netherlands)
- 50 **Novel immunoassay formats for integrated microfluidic circuits: diffusion immunoassays (DIA) [3912-07]**
B. H. Weigl, Micronics, Inc.; A. Hatch, A. E. Kamholz, P. Yager, Univ. of Washington
- 57 **Image reconstruction in tissuelike turbid media under single- and two-photon excitation [3912-08]**
X. Gan, N. Dragomir, M. Gu, Swinburne Univ. of Technology (Australia)
- 64 **OPUS: an optically parallel ultrasound sensor [3912-09]**
J. S. Kallman, A. E. Ashby, D. R. Ciarlo, G. H. Thomas, Lawrence Livermore National Lab.

SESSION 2 CELL- AND PROTEIN-BASED MICRITECHNOLOGY

- 76 **BiOMEMS applied to the development of cell-based bioassay systems [3912-10]**
C. J. Brennan, K. Domansky, P. Kurzawski, L. G. Griffith, Massachusetts Institute of Technology
- 88 **Modular microinstrumentation for endothelial cell research [3912-11]**
B. L. Gray, A. I. Barakat, D. K. Lieu, S. D. Collins, R. L. Smith, Univ. of California/Davis

- 95 **Microchannel arrays with improved accessibility and use for cell studies and emulsification** [3912-12]
Y. Kikuchi, National Food Research Institute (Japan); H. E. Kikuchi, Y. Kuboki, Hokkaido Univ. (Japan); M. Nakajima, National Food Research Institute (Japan)
- 105 **Microfabricated in-vitro cell culture systems for investigating cellular interactions: fabricating a model system for cardiac myocytes** [3912-13]
J. Deutsch, T. A. Desai, D. Motlagh, B. Russell, Univ. of Illinois/Chicago
- 114 **Mechanisms for protein micro-/nano-patterning on photopolymer substrates** [3912-15]
D. V. Nicolau, Swinburne Univ. of Technology (Australia)

SESSION 3 FABRICATION AND CHARACTERIZATION OF BIOMEMS

- 122 **Characterization of fibroblasts and proteins on thin films** [3912-16]
C. S. Giannoulis, T. A. Desai, Univ. of Illinois/Chicago
- 130 **Glass, plastic, and semiconductors: packaging techniques for miniature optoelectronic components** [3912-17]
M. D. Pocha, H. E. Garrett, R. R. Patel, L. M. Jones II, M. C. Larson, M. A. Emanuel, S. W. Bond, Lawrence Livermore National Lab.; R. J. Deri, Terawave Communications Inc.; R. F. Drayton, Univ. of Minnesota/Twin Cities; H. E. Petersen, M. E. Lowry, Lawrence Livermore National Lab.
- 141 **Microspectrometer system for the near-infrared wavelength range based on LIGA technology** [3912-18]
P. Krippner, T. Kühner, J. Mohr, V. Saile, Forschungszentrum Karlsruhe (Germany)
- 150 **Physical characterization of capillary waveguides** [3912-22]
B. Schelle, P. Dreß, H. Franke, Univ. of Duisburg (Germany); K. F. Klein, Fachhochschule Giessen-Friedberg (Germany); J. P. Slupek, Eppendorf-Netheler-Hinz GmbH (Germany)

SESSION 4 ANALYTICAL APPLICATIONS OF BIOMEMS

- 158 **Long-range translation actuator** [3912-20]
A. P. Wallace, D. L. Howard, Univ. of California/Davis; J. Sirota, Joint Ctr. for Earth Systems Technology; R. L. Smith, S. D. Collins, Univ. of California/Davis
- 166 **Determination of ammonia in a flow injection cell using the diode laser/fiber optic colorimetric spectrometer** [3912-21]
S.-H. Kim, S. M. Nam, G. S. Byun, S. Y. Yun, S. Hong, Soonchunhyang Univ. (Korea); J. S. Yoo, Korea Basic Science Institute
- 173 **Selective detection of hydrocarbon vapors by ATR-leaky mode spectroscopy** [3912-24]
R. P. Podgorsek, H. Franke, Univ. Duisburg (Germany); J. G. Woods, Loctite Corp.; R. A. Lessard, COPL/Univ. Laval (Canada)
- 183 *Addendum*
- 184 *Author Index*

SESSION 1

BioMEMS for Diagnostics and Biosensing

Detecting Cancer Quickly and Accurately

P. L. Gourley, A. E McDonald, J. K. Hendricks, G. C. Copeland, J. Hunter, O. Akhil, D. Cheung, and J. Cox
Sandia National Laboratories, Albuquerque, NM 87185

H. Capps, M. Curry, and S. L. Skirboll
University of New Mexico School of Medicine, Albuquerque, NM 87131

ABSTRACT

We present a new technique for high throughput screening of tumor cells in a sensitive nanodevice that has the potential to quickly identify a cell population that has begun the rapid protein synthesis and mitosis characteristic of cancer cell proliferation. Currently, pathologists rely on microscopic examination of cell morphology using century-old staining methods that are labor-intensive, time-consuming and frequently in error. New micro-analytical methods¹⁻⁶ for automated, real time screening without chemical modification are critically needed to advance pathology and improve diagnoses. We have teamed scientists with physicians to create a microlaser biochip (based upon our R&D award winning bio-laser concept) which evaluates tumor cells by quantifying their growth kinetics. The key new discovery was demonstrating that the lasing spectra are sensitive to the biomolecular mass in the cell, which changes the speed of light in the laser microcavity. Initial results with normal and cancerous human brain cells show that only a few hundred cells -- the equivalent of a billionth of a liter -- are required to detect abnormal growth. The ability to detect cancer in such a minute tissue sample is crucial for resecting a tumor margin or grading highly localized tumor malignancy.

1. INTRODUCTION

Cancer is a set of diseases that originate in the genome and its products expressed in the cell. The quantum unit of cancer in the genome progresses from a disease of a single cell to localized tumor to metastatic disease profoundly affecting the entire body. The difficulty in detecting these diseases arises from the subtle onset of the disease in a single cell embedded in a host organ comprising billions of cells. Through recent interdisciplinary scientific research, modern medicine has significantly advanced the diagnosis and treatment of disease. However, little progress has been made in reducing the death rate due to cancer, which remains the leading cause of death in much of the world. Pathologists routinely rely on microscopic examination of cell morphology using methods that originated over a hundred years ago. These staining methods are labor-intensive, time-consuming, and frequently in error. New micro-analytical methods¹⁻⁶ for high speed (real time) automated screening of tissues and cells are critical to advancing pathology and hold the potential for improving diagnosis and treatment of cancer patients.

Novel technologies to assess these diseases in their early development are crucial to effect a successful treatment and recovery. Among the most promising methods for early detection are physico-chemical means for selectively labeling the affected cell and identifying it by quantum mechanical interaction of that cell with electromagnetic or acoustic energy fields (e.g. magnetic, x-ray, laser, ultrasound). The ultimate success of these diagnosis modalities is dependent upon the three dimensional spatial resolution of the interaction volume and the signal strength or sensitivity of the detector.

Promising techniques under investigation include non-invasive but expensive magnetic resonance imaging, inexpensive ultrasound imaging of organs or organ linings, or minimally invasive sampling of minute body tissues or fluids in microdevices. The resolution of MRI imaging is currently in the range of hundreds of microns and limited by the strength of the magnetic field and its gradient. Ultrasound resolution is limited by the wavelength of sound, and is similarly limited to hundreds of microns. Optical and Laser-based spectroscopies and imaging are inherently higher resolution, being limited only by the optical diffraction of light to hundreds of nanometers. Nanoscopic tools like the near-field optical scanning microscope push the resolution to tens of nanometers (the size of protein molecule) and are limited by fiber optic tip microfabrication techniques.

A new set of nanoscopic lasers is emerging from the materials science/laser engineering communities.⁷ The new lasers have ultrasmall dimensions from the nanometer to micrometer scale for confining intense light into an extremely small

interaction volume. These lasers have been shrunk to an astonishing scale of nanometers, even smaller than the wavelength of the light they produce. At such sizes less than one hundredth the thickness of a human hair, curious aspects of quantum physics begin to take over. By exploiting this quantum behavior, researchers can tailor the basic characteristics of the devices to achieve even greater efficiencies and faster speeds. Nanolasers have myriad future applications in optical computers, where light would replace electricity for transporting, processing and storing information, and in fiber-optic communications. Devices for the latter application are now in commercial production. Although these devices are in prototype form, they have already been applied to biomedical research.⁸⁻¹⁰ In preliminary experiments to assess cell structure, the laser has shown the capability to probe the human immune system (caliper cell and nucleus dimensions of lymphocytes),¹⁰ characterize genetic disorders (quantify sickled and normal red blood cell shapes and hemoglobin content),¹⁰ and distinguish cancerous from normal cells.^{8,9}

By teaming experts in semiconductor physics, microfabrication, surface chemistry, film synthesis, and fluid mechanics with microbiologists and medical doctors, we are investigating nanostructured biochips to assess the condition of tumor cells by quantifying total protein content. This technique has the potential to quickly identify a cell population that has begun rapid protein synthesis and mitosis, characteristic of tumor cell proliferation. By incorporating microfluidic flow of cells inside the laser microcavity for the first time, we have enabled high throughput screening of cells in their native state, without need of chemical staining, in a sensitive nanodevice.

2. NEURO-ONCOLOGY

Tumors of the nervous system are generally classified according to cell or tissue of origin. In the revised World Health Organization classification, nine categories are recognized: (1) neuroepithelial tumors, (2) tumors of cranial and spinal nerves, (3) tumors of the meninges, (4) hemopoietic tumors, (5) germ cell tumors, (6) cysts and tumor-like lesions, (7) anterior pituitary tumors, (8) local extensions of regional tumors, and (9) metastatic tumors. Each of these major categories has numerous subcategories. For example, neuroepithelial tumors contain nine subcategories: astrocytic, oligodendroglial, ependymal and mixed glial tumors, choroid plexus tumors, neuroepithelial tumors of uncertain histogenesis, neuronal and mixed neuronal-glial tumors, pineal tumors and embryonal tumors.

At the heart of such classifications is the ability to "grade" tumors. Two major reasons exist for grading brain tumors: (1) to establish relationships between various entities allowing communication between people, and (2) to predict the prognosis of a patient with a particular tumor. Grading of tumors is often less than ideal because we use standard histological techniques to define relatively few tiers onto a biological system that is dependent on multiple nonhistological aspects such as the inherent biology of the tumor. Newer techniques to further describe and distinguish cells of a tumor versus normal brain cells are vital to potentially improving on the current grading schemes.

Normal human astrocyte (NHA) cells¹¹ are star-shaped process-bearing cells distributed throughout the central nervous system. They constitute from 20 to 50% of the volume of most brain areas and come in two forms, protoplasmic and fibrous types predominant in gray and white matter, respectively. Some of these cells serve as scaffolding for the migration of neurons and play a critical role in defining the cytoarchitecture of the central nervous system. Astrocytoma is a term given to tumors comprising astrocytes with a relatively well-differentiated histological appearance. Glioblastoma multiforme¹² (GBM) is a term given to tumors which are the least differentiated and most aggressive form of astrocytoma. It accounts for about 20% of all primary intracranial tumor cases. In the studies described in this paper, we have used cultured normal human astrocytes from gray matter and glioblastoma cells as representative cells from normal and cancerous tissue, respectively. These two cell types are the first candidates for realtime analysis of brain cells in the microcavity laser.

Real-time analysis of cells in brain tumors not only allows for more timely conclusions on the final diagnosis, but has the potential to assist the neurosurgeon in the operating room. For example, the accuracy of brain biopsies could be verified in the operating room without waiting for the pathologist to process the tissue for a preliminary and sometimes inaccurate diagnosis. Even more important may be capacity for real-time analyses to aid in the actual tumor resection. Multiple studies have shown the benefit of total resection (versus near total resection) in patient survival, and time to tumor recurrence for a variety of brain and spinal tumors, many of which do not typically manifest well demarcated margins with normal tissue. An ideal surgical tool would utilize an extremely sensitive and efficient method to inform the neurosurgeon immediately that the resection cavity still contains more tumor cells despite the gross appearance of total resection.

3. NANOLASER/MICROFLUIDIC BIOCHIP FOR ANALYZING TUMOR CELLS

We have recently developed a microfluidic system (see Fig. 1) that incorporates a nanolaser chip for high throughput analyses of flowing biofluids.⁸ The semiconductor nanolaser is the enabling component of this microanalysis system because of its ability to emit coherent, intense light from a small aperture compatible with the dimensions of a human cell. By using a surface-emitting semiconductor geometry, we were able to incorporate fluid flow inside a laser microcavity for the first time. This confers significant advantages for high throughput screening of cells, particulates and fluid analytes in a sensitive microdevice. As these fluids flow through these channels, their components will alter the emitted lasing spectrum. The spectral shifts in the lasing frequencies can then be used to measure the protein concentration in the cells.

Most importantly, cells can be analyzed in their physiologic condition as removed from the body. There are no time delays or difficulties associated with tagging cells with stains or fluorescent markers. Thus, the usual time delay of tissue pathology under the microscope is eliminated. And, the lasing technique has been found to detect subtle changes in cellular compositions that are orders of magnitude smaller than can be observed by standard optical microscopy. In addition, this device does not alter or manipulate the cellular components, thus allowing for direct observations of nuclear and cellular events.

The applications of such a portable biological sensing device are far-reaching. One surgical application of this biocavity laser is a "smart scalpel," for online flow cytometry in the operating room. Conventional flow cytometers tend to be large, expensive instruments that require highly trained personnel for tagging the cells and operating the instrument. A portable cytometer system designed for an operating room setting could analyze minute volumes of cells and improve the success rate of tumor resection. Such a system could decrease costs and improve patient survival rates by avoiding tumor regrowth and subsequent surgeries. To achieve this capability it is necessary to understand the basic operation of the laser and its ability to detect biologically relevant events.

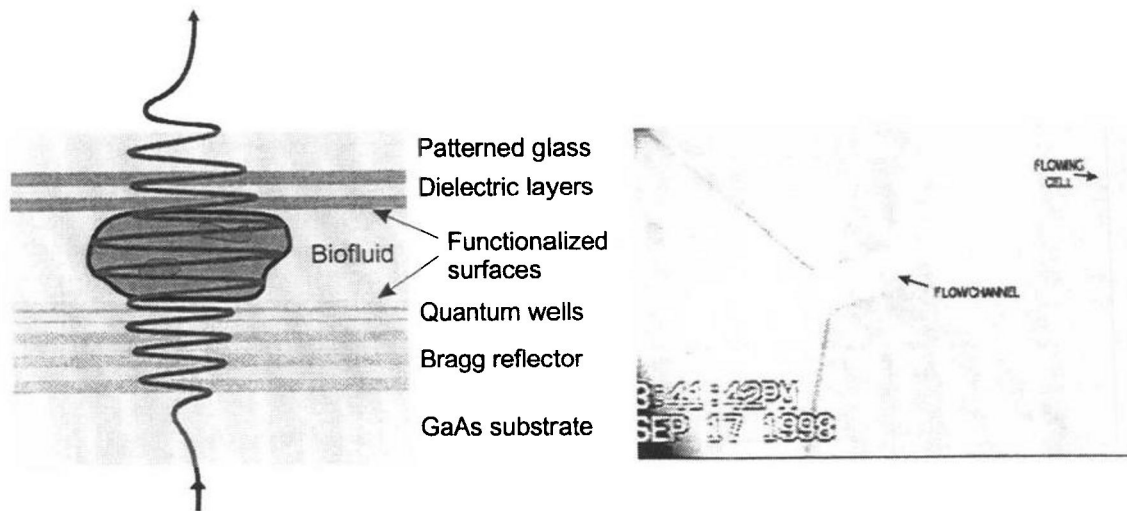


Fig. 2 Left schematic diagram shows microcavity laser in which cells are analyzed. The cells are flowed through the cavity (video micrograph on right hand side) and trigger the onset of lasing. The spectral components of the output beam are analyzed in real time to measure the biochemical makeup of the cells.

3.1 Biomolecular concentration measurements for studying the cell cycle

The biocavity laser spectrum provides a quantitative measure of total biomolecular concentration in the cell. This measurement can be explained as follows. Typical mammalian cells are composed of water (70%), proteins (18%), lipids (5%), metabolites (3%), sugars (2%), and RNA/DNA (1-2%).¹³ Simpler molecules like H₂O and sugars comprise chemical bonds that have weaker dipole oscillator strengths in the UV absorption spectrum and contribute less to the refractive index in the spectral region 850 nm where the laser operates. On the other hand, more complex molecules like protein and RNA/DNA comprise many carbon-carbon and carbon-nitrogen double bonds and have strong oscillator strengths in the UV absorption spectrum. These optical absorptions give rise to strong enhancements of the refractive index at longer wavelengths.¹⁴ Since the proteins are the most abundant complex molecule in the cell, and since the complex molecules contribute most strongly to the refractive index, the lasing spectrum is most sensitive to the protein content of the cell.

When a liquid is flowed through the laser microcavity, optical resonance occurs when the roundtrip light path is an integral number of light wavelengths. These resonance conditions appear as sharp peaks in the emission spectrum of the laser. When a cell comprising a biomolecular concentration is placed in the laser, the resonance peaks are shifted to longer wavelengths and can be precisely measured with a spectrometer. By knowing the specific refractive increment (the index change for a given concentration of molecules), the average biomolecular concentration can be directly inferred from the spectral shift of the peaks. Since many molecules are present, and each contributes to the refractive index, the measurement represents an average biomolecular concentration within the cell.

It is feasible to use the biomolecular concentration to assess the stages of the cell cycle (illustrated in fig.2 left side), and to identify possible failures in regulation of the cycle. During interphase, the cell must reproduce genetic material and the other protein components before it undergoes mitosis and cytokinesis.¹³ It is during this period that the cell is most active in transcribing and translating genetic information. G1 is a gap phase in the cell cycle where there is gene expression and biochemical activity, but no replication of DNA. In the S phase, the nucleus replicates its chromatin and cellular proteins. Thus the amount of DNA and protein must double. G2 is a second gap phase in the cell cycle that follows the S phase. During G2 the cell is a resting phase before it proceeds to divide by mitosis. Most cells spend very little time in G2, so few cells would be found in this phase. On the other hand, irregular cell cycles induced by oncogenes or other perturbations would alter the relative population of cells found in G1 and G2 phases. By measuring biomolecular concentration (or biomolecular mass in a fixed cell volume), it is possible to quantify the number of cells in G1 and G2 and assess the cell growth rate.

The cell grows by absorbing nutrients through the membrane from surrounding media. The uptake of biomolecular mass is thus proportional to the membrane area. On the other hand, the volume grows as the 3/2 power of the area. Thus the biomolecular concentration (mass over volume) must decrease as the inverse square root of the area, during the initial growth of the cell. At some point, the cell volume must fix and then the biomolecular concentration can increase. The concentration increases significantly during synthesis phase because the DNA must replicate. During DNA replication it is likely that protein replication occurs almost simultaneously through normal transcription and translation. As a consequence, the concentration will approximately double as the cells enter G2. It is unlikely that the cell volume will increase significantly during synthesis, since this would necessitate a reduction in concentration and decrease replication rate. Only after mitosis when the genes are functional, would the cell volume be expected to increase.

The biocavity laser wavelength shift measures the difference in cell biomolecular concentration relative to the surrounding media, since it depends on the relative index of refraction of the cell and media. Thus the laser can track the changes in concentration during the cell cycle. The concentration c (or mass m for a fixed volume) is a function of time as $c(t)$. The function must have the following characteristics illustrated in Fig. 2 (right side inset): it must start at a finite value c_0 after mitosis and grow slowly until time T_1 the end of G1. During synthesis c must increase abruptly before finalizing at approximately $2c_0$ at T_1+T_s . Then, c must be relatively constant for a time T_2 until mitosis. In a population of cells, the probability of finding a cell with a particular c will be inversely proportional to the dc/dt . So, the relative number of cells in G1 will be $T_1/\int c_1$ where $\int c_1$ is the small increase in c during G1. In S the number is T_s/c_0 and in G2 it is $T_2/\int c_2$. The concentration (mass) and probability are shown on the right hand side of Fig. 2. Most of the cells are found in G1, and cells spend very little time in G2, so few cells are normally found here. However, oncogenes shorten G1 and increase the number of cells in G2. These changes are observable with the biocavity laser.

The replication kinetics of a single cell can be inferred from the distribution of cells in a population

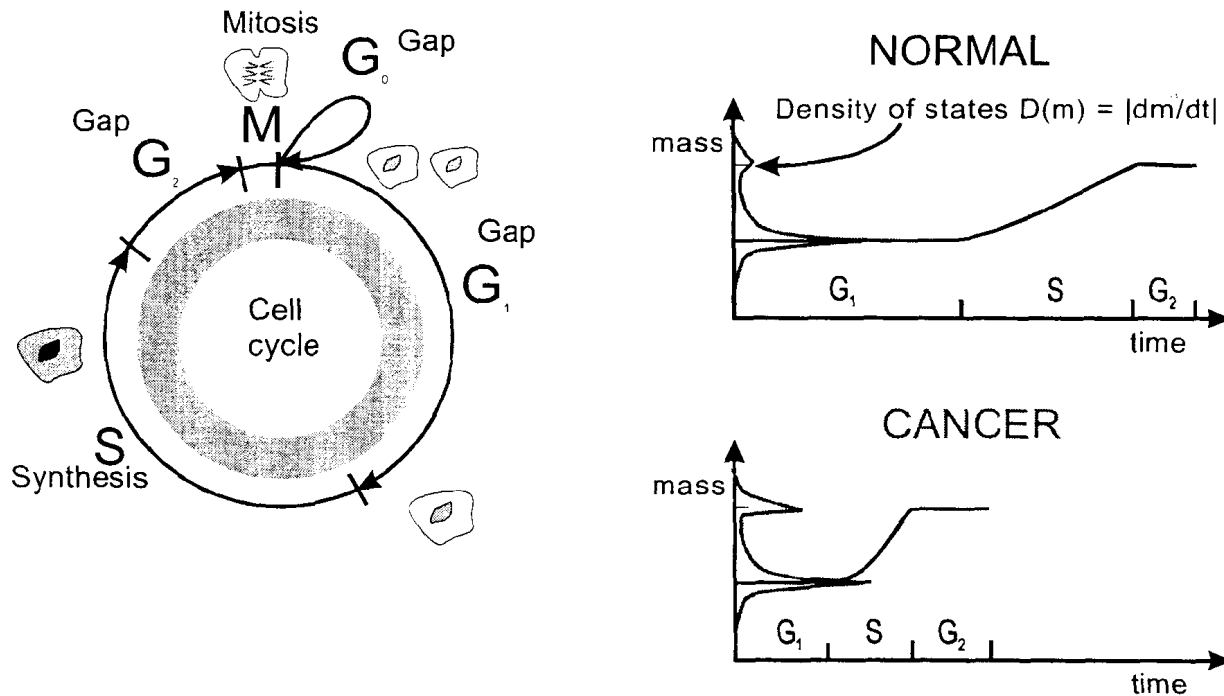


Fig. 2. Left diagram shows the cell growth and replication cycle, including mitosis M when the cell divides, a dormant gap phase G₀, growth and regulation gap phase G₁, synthesis phase S, and final gap phase G₂. The top right diagram shows how the protein mass of the cell doubles with time during the normal cell cycle. Cells in a population are distributed in phase according to the duration of the phase (red curve showing most cells in G₁ phase). The bottom right diagram shows the growth curve for cancer cells that exhibit a shortened G₁ phase and a larger percentage of cells in the G₂ phase.

3.2 Results for Normal and Cancerous Brain Cells

Figure 3 (left) shows a histogram of spectral shifts for a population of normal human astrocytes. The main peak near 4.5 nm is assigned to cells in G₁, comprising 98% of the population. The smaller peak near 9 nm is assigned to the remaining 2% of cells in G₂. This distribution of cells indicates that the cells are growing slowly with two well-defined population groups. Figure 3 (right) also shows results for glioblastoma cancer cells and reveal two subpopulations at 5 and 10 nm shifts corresponding to G₁ and G₂ phases. Here, there are considerably more cells (~5%) in the G₂ phase. Further, the population is much more broadly distributed between the two phases, indicating many intermediate cells in the synthesis phase. These data indicate that the glioblastoma cells are proliferating at a much higher rate than the normal astrocytes, as expected for tumor cells. This observation is consistent with the measured rate of cell growth in culture and conventional flow cytometry data using protein markers in tumor cells.

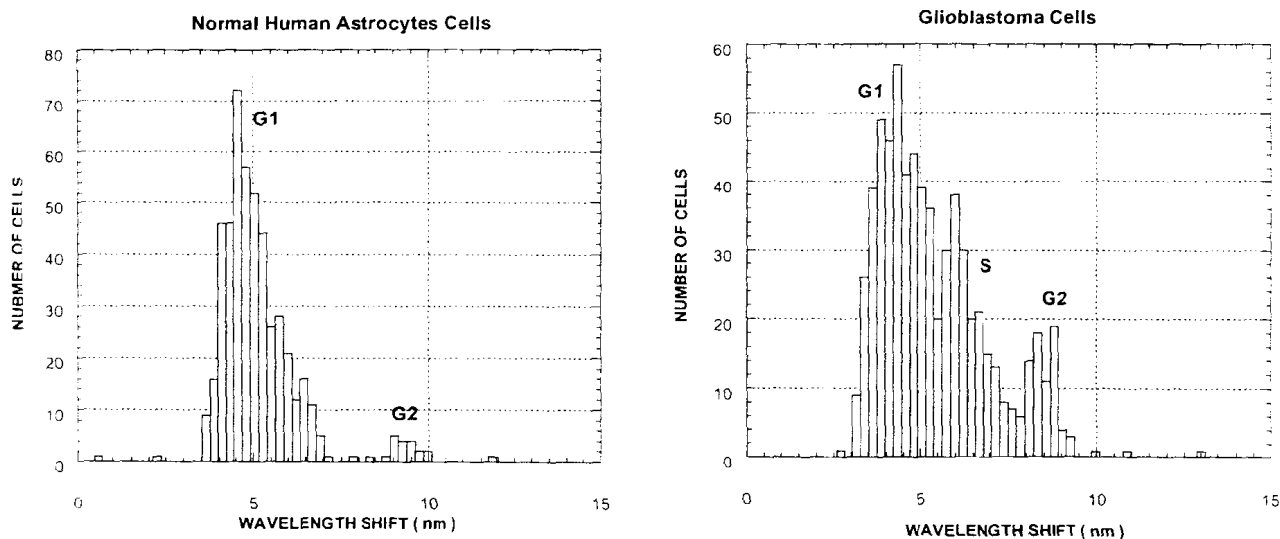


Fig. 3. Histograms for normal human astrocytes (left) and glioblastoma cells (right) showing the distribution of cells in wavelength shift of the laser line relative to the microcavity with fluid but without the cell. The wavelength shift is approximately proportional to the total biomolecular concentration in the cell and proteins are the major biomolecular component.

To check the identity of the G1 and G2 peaks, we used conventional flow cytometry to sort a mixed population of GBMs into G2 cells. The unsorted and sorted cell suspensions were flowed through the microcavity. The results are shown in Fig. 4. The left hand figure is the unsorted suspension comprising G1 cells that exhibit a broad peak near 5 nm and G2 cells that exhibit a peak near 10 nm. The right hand figure shows the corresponding histogram for the sorted G2 cells. This data reveal only a sharp peak near 10 nm. Thus, it is clear that the microcavity spectral peaks correspond to the G1 and G2 peaks observed with DNA tagging in conventional flow cytometry.

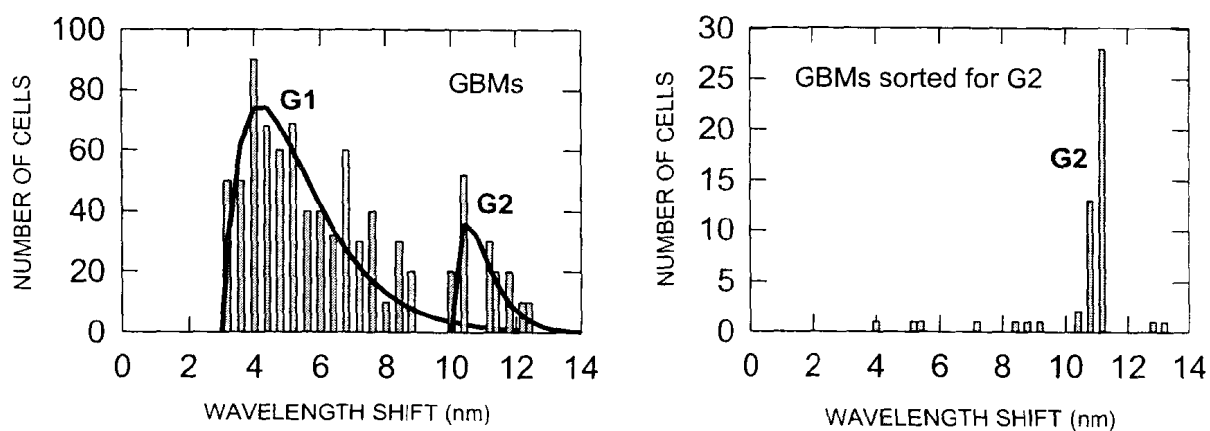


Fig. 4. (a) left figure: microcavity histogram of unsorted G1 and G2 glioblastoma cells from culture. The data reveal prominent features centered near 5 and 10 nm, respectively, associated with G1 and G2 phases of the cell cycle. The solid lines are theoretical fitting functions of the form $I \propto \exp(-a/c)$, where a is proportional to c . (b) right figure: microcavity histogram of G2 cells that had previously been sorted by a conventional flow cytometer using DNA fluorescent tags. Here, only a sharp peak near 11 nm is observed for the G2 cells.

In the figure, we have also analyzed the shape of the peaks by fitting them with a theoretical function (solid line). The fitting function is the probability of finding a cell with a given biomolecular concentration c at a temperature T surrounded by a solution of concentration c_0 . An osmotic pressure develops within the cell because the membrane acts as semipermeable barrier between the cytosol and the exterior. The pressure is given by $P=(c-c_0)kT$ which is the van't Hoff relation.¹⁵ The net energy to raise the concentration from c_0 to c against the diffusive force is PV where V is the cell volume. If an ensemble of cells was treated in analogy to a population of particles in thermal equilibrium, the chemical potentials of the cytosols of each cell would be equal to the chemical potential of the exterior solution. In this case the differential probability of finding a cell with energy E is proportional to $\exp(-E/kT)$. The probability distribution would take the form $f(c)\exp(-cV)$. We have fitted the data to this functional form and found a best fit (solid line in fig. 4) of $\lambda \exp(-\lambda cV)$, where λc is proportional to λ . This function features a sharp onset at low λ and an exponential tail at high λ as observed in the data of fig. 4.

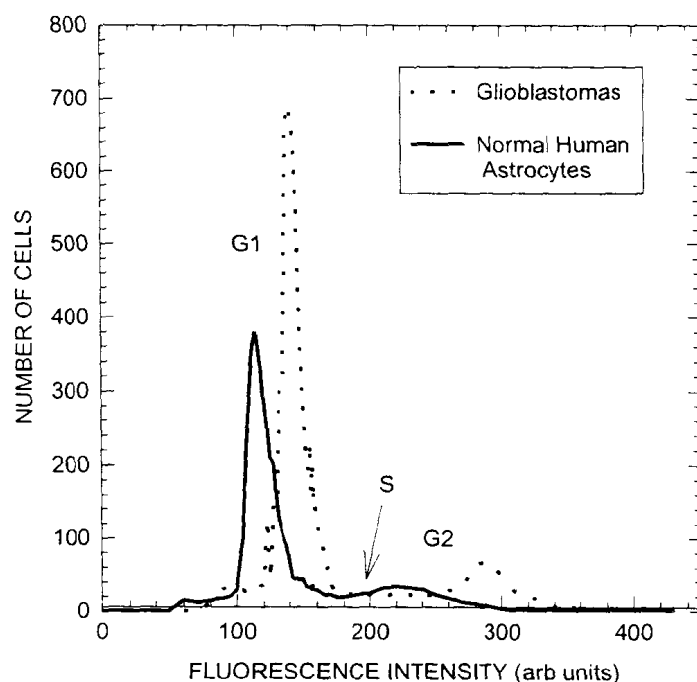


Fig. 5. Typical histograms of DNA fluorescent intensity recorded by conventional flow cytometry with normal human astrocytes (dashed lines) and glioblastoma cells (solid lines). Both curves reveal major G1 subpopulations and minor G2 subpopulations.

Fig. 5 shows typical histograms of DNA fluorescent intensity recorded by conventional flow cytometry with normal human astrocytes (dashed lines) and glioblastoma cells (solid lines). Both curves reveal major G1 subpopulations and minor G2 subpopulations. The intensities of the G2 peaks are exactly double the intensities of the G1 peaks for a given cell type. This is expected if the synthesis process exactly replicates the DNA. Note however, that the ratio G2/G1 increases for GBM cells as expected for enhanced replication rate. Also note the amount of DNA is increased by some 15% in the GBM cells, probably due to extra DNA arising from mutated replication. These observations of DNA content are similar to the data obtained with the biocavity laser for total biomolecular concentration (primarily protein), except that the protein content appears about 15% smaller in the GBM case.